Neutrino oscillations: the rise of the PMNS paradigm

Stéphane Lavignac

IPhT, CEA Saclay, 91191 Gif-sur-Yvette CEDEX, France

Marco Zito

IRFU/SPP, CEA Saclay, 91191 Gif-sur-Yvette CEDEX, France

Abstract

This is the abstract

Keywords:

1. Introduction

Introduction

2. Theory and phenomenology of oscillations 15 pg SL

2.1. Preliminary

Lagrangian NC and CC, nu in SM, m ?

2.2. Basis

U PMNS : D vs M, oscillation independent of D/M vacuum N=2 N=3

2.3. matter

n=const $\rightarrow$ MH determination

2.4. MSW

adiabatic regime

2.5. CP violation

CP violation vacuum (+ CP with matter ?)

3. Oscillation parameters: current status 30pg

3.1. The solar sector: SK, SNO, KamLAND (SL)

reactions + spectrum nu solar (plot)

Davis first indication deficit Ga/Sage confirmation, E dependance

SK mesure spectrum vs E plot

SNO mesure NC/CC → Phi (nu other)/Phi(nue) plot

Kamland confirmation artificial beam (vacuum) E/L oscillation plot precision meas. Dm**2 → excludes LOW → LMA

(MSW interpretation) Borexino mesure various components of the spectrum (Be, CNO) → confirmation MSW (upturn) day night effect

ref

3.2. The atmospheric sector (MZ)

In this subsection we will describe the status of the so called atmospheric neutrino oscillations, i.e. the 3-2 oscillations that were first discovered in the study of atmospheric neutrinos and later were precisely measured with the use of long baseline neutrino beams.

3.2.1. The atmospheric neutrino flux

The atmosphere is constantly bombarded by primary cosmic rays, composed mainly of protons, with a smaller component of α particles and heavier nuclei. The interaction of these particles with atomic nuclei in the atmosphere produces hadronic showers composed mainly of pions and kaons. The decay of these mesons according to $\pi^+ \to \mu^+\nu_\mu$ followed by $\mu^+ \to e^+\nu_e\bar{\nu}_\mu$, $K^+ \to \pi^+\nu_\mu$ and $K_L \to \pi^+e^-\nu_e$ together with their charge conjugated processes, produces a flux of ν_μ and ν_e with a steeply falling power-law spectrum (Fig. 1).

The calculation of this neutrino flux [11] relies on the knowledge of the primary flux and composition, of the Earth magnetic field, and of the hadro-production cross-section. Recent studies [12, 6, 7] taking into account 3D effects and recent measurements of the hadro-production cross-sections largely improve on previous efforts and reach precisions of 7-8 % for the flux in the 1-10 GeV range. It should be noticed that the ratio $N(\nu_\mu + \bar{\nu}_\mu)/N(\nu_e + \bar{\nu}_e)$ is predicted with a much better precision of a few % as several systematic uncertainties cancel in this ratio. In the limiting case where all the muons from pion decays decay themselves in flight, this ratio is close to 2, as can be easily deduced from the decay processes mentioned above.

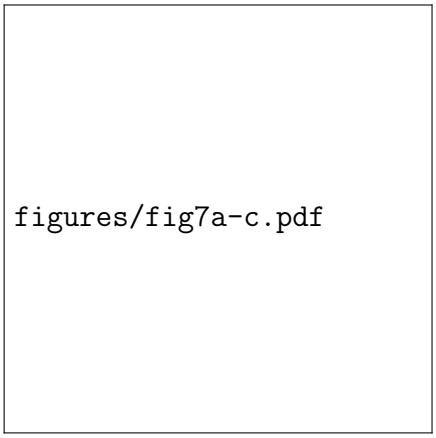

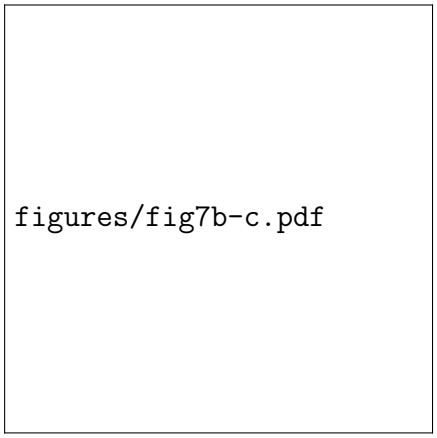

Figure 1: The flux of atmospheric neutrinos (left) and several flux ratios (right) [12].

3.2.2. The early days, the up-down asymmetry and controversy

The study of atmospheric neutrinos started in the 1960: two experiments in very deep mines, in South Africa [15] and in India [3], observed muons produced by their interactions. In the 1980, several massive underground experiments, mainly motivated by the search for the proton decay predicted by Grand Unification theories, started collecting data. These experiments needed to study in detail atmospheric neutrino interactions as they constitute a background for proton decay searches.

In 1988, Kamiokande reported a deficit in the number of ν_μ of events, while the number of ν_e events agreed with the prediction. This started the so-called atmospheric neutrino anomaly. This deficit was also observed by the IMB experiment and later by MACRO and SOUDAN-2, while Fréjus and NUSEX observed no deficit.

3.2.3. The evidence for atmospheric neutrino disappearance

The situation evolved rapidly with the advent of Super-Kamiokande, that started data-taking in 1996. Super-Kamiokande is very large water Cherenkov detector located in the Mozumi mine (Gifu prefecture, Japan), under a 1000 m rock overburden, equivalent to 2700 m of water. It is a stainless steel tank (41.4 m high, 39.3 m diameter) containing 50 kt of ultra-pure water. The detection volume is partitioned in an outer detector, composed of 1885 8 inch PMTs, and an inner detector with 11146 20 inch PMTs. The fiducial volume is 22.5 kt. Super-Kamiokande could rapidly accumulate a rather large data set of atmospheric neutrinos, measuring the direction of

the produced lepton, its energy for fully contained events and their nature. Above a few hundred MeV/c, the direction of the produced lepton is strongly correlated to the direction of the incoming neutrino.

In 1998, the Super-Kamiokande collaboration presented their first analysis of atmospheric neutrinos [10], in particular the distributions of zenith angle for ν_μ and ν_e event selections (see Fig. 2 for an updated distribution) based on 33 kton year. This was the first compelling evidence for neutrino oscillations as the explanation of the previously mentioned anomaly.

Indeed the neutrino path from the production to the detection varies from 15 km for down-going neutrinos (cosine of the zenith angle equal to 1) to more than 12000 km for up-going neutrinos having traversed the whole Earth (cosine of the zenith angle equal to -1), thereby probing a large span of possible oscillation lengths.

In a two neutrino scenario, the ν_μ disappearance is governed by $\sin^2(2\theta)\sin^2(4\Delta m^2 L/E)$, where θ is the relevant mixing angle and Δm^2 the squared-mass difference of the mass eigenstates. A glance at Fig.2 reveals several important overall features:

- there is a strong disappearance of ν_μ, especially visible for up-going neutrinos. As the survival probability for very long baseline approaches $1/2\sin^2(2\theta)$, and the observed survival probability is close to 0.5, the mixing angle is therefore close to the maximal value $\pi/4$.

- The disappearance sets in for neutrinos close to horizontal zenith angle, and therefore the oscillation length should be of the order of 400 km for energy around 1 GeV, or $\Delta m^2 \simeq 10^{-3}\mathrm{eV}^2$.

- There is no sizeable excess or deficit of ν_e. Therefore the oscillations of ν_μ should mainly involve either $\nu_\mu \to \nu_\tau$ or $\nu_\mu \to \nu_s$, where ν_s is an additional neutrino state.

Independently of any accurate predictions of the neutrino flux, the experimental observation of the distributions of Fig.2 is sufficient to make a strong case for neutrino disappearance. Indeed, above several GeV, the neutrino flux is isotropic, as the primary cosmic rays are not deflected in a significant way by the geomagnetic field. The observation of a zenith angle dependent deficit of the neutrinos is then a sufficient argument to conclude that these neutrinos undergo a non-standard propagation.

While in 1998 other hypotheses like decay or decoherence were still open, more recent data from long baseline accelerator experiments have ruled out

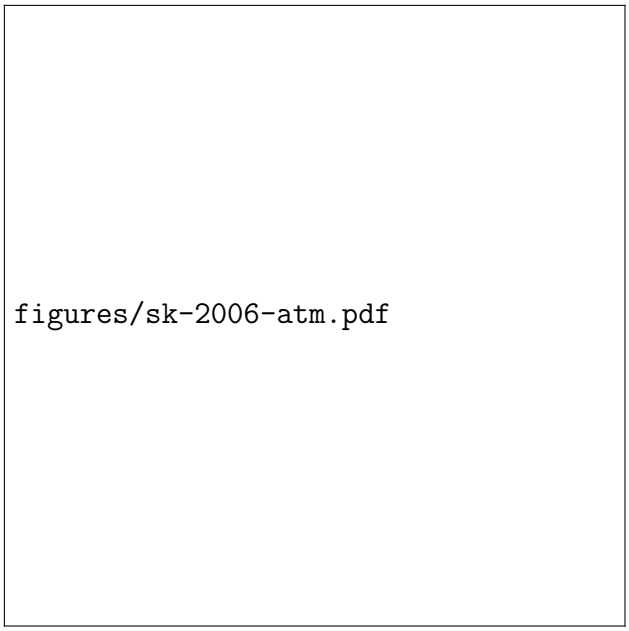

Figure 2: Zenith angle distributions of Super-Kamiokande atmospheric neutrino events from [13]. Fully contained e-like, μ-like events are shown for data (filled circles with statistical error bars), MC distributions without oscillation (boxes) and best-fit distributions (dashed). The box height shows the statistical error.

all explanations apart from oscillations because the alternative hypotheses imply a different L/E behaviour.

The IceCube experiment at the South Pole has recently completed the installation of DeepCore, a denser array of optical modules, aimed at significantly lowering the muon threshold. With data recorded between 2011 and 2014, corresponding to 5074 observed events, they have recently published an analysis of the disappearance of atmospheric ν_μ [1] in the range 10-100 GeV, requiring the zenithal angle to satisfy $\cos theta < 0$, which has a similar sensitivity to that of Super-Kamiokande (Fig. 3) with the prospects of further improvements.

Figure 3: Distribution of atmospheric neutrino events measured by the IceCube experiment[1] as a function of reconstructed L/E. Data are compared to the best fit and expectation with no oscillations (top), and the ratio of data and best fit to the expectation without oscillations is also shown (bottom). Bands indicate estimated systematic uncertainties.

3.3. Long-baseline neutrino beams

Neutrino beams [14] based on particle accelerators have been used since the 1960s, when they provided the evidence for the existence of two types of neutrino, ν_e and ν_μ. The general design is based on a high intensity

proton beam impinging on a target and producing pions and kaons through interactions on the target nuclei. These mesons decay in a dedicated volume downstream of the target, creating mainly a ν_μ beam.

The long baseline beams are based on the so called wide band beam concept. Here the secondary charged mesons are focused using a system of magnetic devices, called horns. The horns, usually with a cylindrical symmetry around the beam, are pulsed with a very intense current in coincidence with the arrival of the beam.

The flux is tuned in such a way that the phase $\Delta m^2_{32} L/(4E)$ reaches $\pi/2$ for the design baseline L and the peak energy E, in order to probe the atmospheric oscillation sector with the beam ν_μ. To do so, the proton energy, the target length and width, the focussing system and the decay volume length and width need to be accurately designed and optimized.

An off-axis neutrino beam [8] relies on the following idea: as the ν_μ are mainly produced by the two-body decays of pions, there is a correlation between pion energy E_π, the neutrino energy E_ν and the decay angle θ

$$E_\nu = \frac{(1 - (m_\mu/m_\pi)^2) E_\pi}{(1 + \gamma^2 \theta^2)} \tag{1}$$

valid in the limit of small angles.

Neutrinos emitted at a small angle with respect to the pion direction have a distinct narrow spectrum peaking at a much lower energy with respect to the on axis beam. This feature that has been used by the T2K and NOvA experiments, offers several advantages because it avoids the large high energy tail of the on axis beam, thereby reducing some background reactions.

As the neutrino beam is a tertiary beam, it is necessary to include in the experimental apparatus monitoring devices to ensure that it is stable in intensity and direction. To this effect, muon detectors, sensitive to the muons produced by the pion decays, are placed close to the end of the decay volume. Moreover, as the neutrino flux and cross-sections and the beam composition are not known with sufficient precision, a near detector is located close to the target station (typically within a few hundred meters). The near detector constrains the neutrino interaction rate, proportional to the product t=of neutrino flux and the cross-section. Moreover, the near detector allows to measure the beam composition and to perform study of several neutrino cross-section.

Description of T2K beam line if space allows.

Figure 4: Neutrino energy as a function of the pion energy for on-axis decays and several off-axis angles. For a non-zero off-axis angle, the neutrino energy reaches a maximum. This feature is currently exploited in the T2K and NOvA experiments.

Exp.	Energy (GeV)	Power (kW)	L (km)	FD mass (kt)	POT
K2K	30		250	22.5	
MINOS	120	700	790	5.4	
OPERA	450	732			$1.8\ 10^{20}$
T2K	30	750	295	22.5	$8\ 10^{21}$
NOvA	120	700	810	14	
HK	30				
DUNE	120	1200	1300	40	

Table 1: Parameters of recent and future long baseline experiments. Energy and power refer to the primary proton beam, L is the baseline, FD the mass of the far detector. POT (Proton On Target) represents the integrated dataset as of 2016.

3.3.1. Results from long-baseline accelerator experiments K2K MINOS T2K NOVA

K2K (KEK-to-Kamioka) was the first long baseline neutrino beam, using Super-Kamiokande as its far detector at 290 km from the neutrino production. Operating between 1999 and 2004, it has measured the disappearance of ν_μ: 112 events were observed, while $158.1^{+9.2}_{-8.6}$ were expected without oscillation, a 4.3 σ effect [5]. This measurement has confirmed neutrino oscillation as the explanation for the atmospheric neutrino disappearance.

Further precision measurements of the $\nu_\mu \to \nu_\mu$ were reported by MINOS, T2K and NOvA.

We will here describe in some detail the T2K measurement, the most precise for what concerns the θ_{23} angle.

Figure 5: Reconstructed ν_μ energy spectrum by the T2K collaboration for data, best-fit prediction, and unoscillated prediction. Bottom: Ratio of oscillated to unoscillated events as a function of neutrino energy for the data and the best-fit spectrum.

3.3.2. Evidence for ν_τ appearance

The OPERA experiment on the CERN to Gran Sasso neutrino beam, taking data between 2008 and 2012, was designed to test the $\nu_\mu \to \nu_\tau$ appearance hypothesis. The detector is based on the Emulsion Cloud Chamber

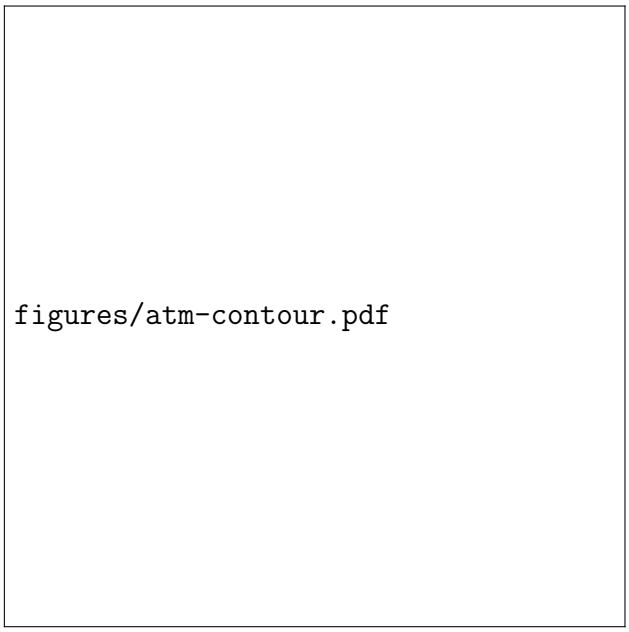

Figure 6: 90% CL regions in the plane Δm^2 versus $\sin^2(2\theta_{23}$ determined by Super-Kamiokande and IceCube-DeepCore using atmospheric neutrinos, and MINOS and T2K using long baseline neutrino beams.

technique, with 1800 ton of nuclear emulsion detectors in the forms of bricks, each brick being composed of a stack of nuclear emulsion film and lead plates. This target, capable of sub-micrometric track resolution, is devoted to the study of the neutrino interaction vertex and the particles associated to it. The identification of the τ leptons relies mainly on their characteristic kink (Fig. 7) due to the decay $\tau \to h\nu_\tau$, or $\tau \to l\nu_\tau\bar{\nu}_l$, where h is a charged meson, and l is an electron or a muon. Another signature is related to the decay $\tau \to 3h\nu_\tau$ where the short τ track ends in a three-pronged vertex. The target detectors are complemented by scintillator trackers and muon spectrometers.

OPERA has observed 5 ν_τ candidate events [4] with a total background of 0.25 ± 0.05 events, mainly coming from decays of charmed particles. This corresponds to a 5.1 σ observation of ν_τ production in an oscillated ν_μ beam.

The Super-Kamiokande collaboration has also searched for ν_τ appearance in multi-ring events to test the hypothesis of $\nu_\mu \to \nu_\tau$ oscillations [2]. While the selected sample is affected by large backgrounds, there is an excess of tau-like events in the upward-going direction with a significance of 3.8 σ, offering a complementary confirmation of the OPERA result.

3.4. The 1-3 sector (MZ)

Solar and atmospheric results are well described by two-flavour mixing models, but we know that there are at least three neutrino flavours and therefore at least three mass eigenstates. The experiments described so-far, while giving robust evidence for neutrino oscillation, do not provide a full picture of 3x3 mixing models.

In order to fully establish the PMNS matrix it is necessary to measure the last mixing angle, θ_{13}. A non-zero value of θ_{13} is required to have CP violation in the lepton sector. The parameter θ_{13} can be measured by reactor neutrino experiments through the measurement of $\overline{\nu}_e$ disappearance at short baselines ($\sim 1\ km$) or by long-baseline accelerator experiments by looking for electron neutrino appearance in the ν_μ beam. Reactor experiments directly measure θ_{13} by observing $\overline{\nu}_e$ disappearance according to the simple equation:

$$P(\overline{\nu}_e \to \overline{\nu}_e) = 1 - \sin^2 2\,\theta_{13} \sin^2(1.267\Delta m^2_{13} L/E) \qquad (2)$$

This is not the case in long-baseline accelerator experiments for which the ν_e appearance probability is a sub-leading effect of the oscillation involving Δm^2_{32} in which ν_μ mainly oscillate into ν_τ. The general expression for $P(\nu_\mu \to \nu_e)$ is a complicated formula that can be derived considering the formalism

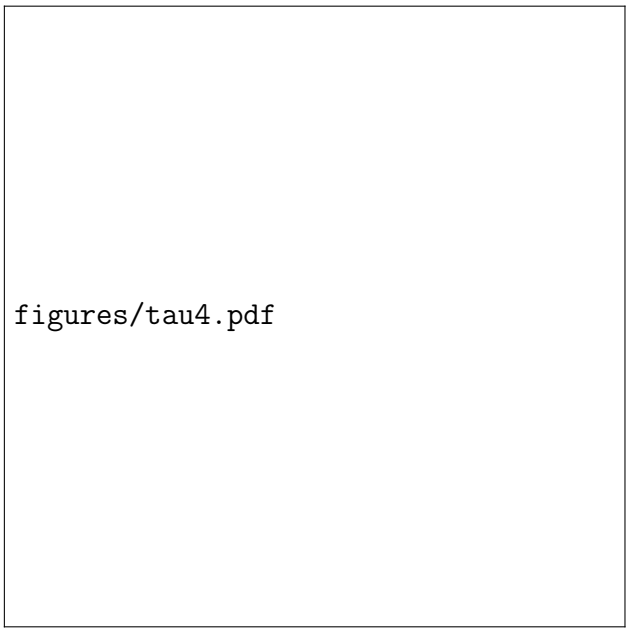

Figure 7: Event display of the fourth ν_τ candidate event from the OPERA experiment [9] in the horizontal projection longitudinal to the neutrino direction. The primary and secondary vertices are indicated as V_0 and V_1 , respectively. The kink between the parent and daughter track, a feature of τ lepton decays, is clearly visible. The yellow stubs represent the track segments as measured in the emulsion films.

for the three neutrino families and depends on a combination of θ_{13}, $\delta_{\rm CP}$ and matter effects due to the large amount of matter crossed by neutrinos before reaching the detector. An approximated expression of this probability is:

$$\begin{aligned} P(\nu_\mu \to \nu_e) &= 4C_{13}^2 S_{13}^2 S_{23}^2 \sin^2\phi_{31} \\ &+ 8C_{13}^2 S_{12}S_{13}S_{23}(C_{12}C_{23}\cos\delta_{\rm CP} - S_{12}S_{13}S_{23})\cos\phi_{32}\sin\phi_{31}\sin\phi_{21} \\ &- 8C_{13}^2 C_{12}C_{23}S_{12}S_{13}S_{23}\sin\delta_{\rm CP}\sin\phi_{32}\sin\phi_{31}\sin\phi_{21} \\ &+ 4S_{12}^2 C_{13}^2(C_{12}^2C_{23}^2 + S_{12}^2S_{23}^2S_{13}^2 - 2C_{12}C_{23}S_{12}S_{23}S_{13}\cos\delta_{\rm CP})sin^2\phi_{21} \\ &- 8C_{13}^2 S_{13}^2 S_{23}^2 \frac{aL}{4E_\nu}(1-2S_{13}^2)\cos\phi_{32}\sin\phi_{31} \\ &+ 8C_{13}^2 S_{13}^2 S_{23}^2 \frac{a}{\Delta m_{13}^2}(1-2S_{13}^2)\sin^2\phi_{31} \end{aligned} \tag{3}$$

where $C_{ij} = \cos\theta_{ij}$, $S_{ij} = \sin\theta_{ij}$ and $\phi_{ji} = \Delta m_{ji}^2 L/4E_\nu$. The terms that include a are a consequence of the matter effects with $a = 2\sqrt{2}G_F n_e E_\nu = 7.56\times 10^{-5}[eV^2](\rho/(g/cm^3)(E_\nu/GeV)$. The term proportional to cos$\delta_{\rm CP}$ is invariant for ν and $\overline{\nu}$ whilst the term proportional to sin$\delta_{\rm CP}$ change if CP is violated. The equivalent term for $P(\overline{\nu}_\mu \to \overline{\nu}_e)$ can be obtained by reversing the signs of the terms proportional to sin$\delta_{\rm CP}$ and to a.

These formulas clearly show the complementarity between reactor and long-baseline experiments. The combination of $\overline{\nu}_e$ disappearance from reactors with the measurement of ν_e (and eventually $\overline{\nu}_e$) appearance in long baseline experiments allows to break the degeneracies and access independentely to θ_{13}, $\delta_{\rm CP}$ and the sign of a.

In this section we will describe the measurements of $\overline{\nu}_e$ disappearance from Daya Bay, RENO and Double Chooz. In addition the combination with measurement of $\overline{\nu}_e$ disappearance provided by The difference between the two channels clearly show the complementarity between reactor and accelerator experiments that can be combined together to measure $\delta_{\rm CP}$ and mass hierarchy.

3.5. Measurements of θ_{13} in reactor experiments

reactor flux

Bugey et al no disappearance

CHOOZ : theta13 small

DCHOOZ RENO Daya Bay theta13 prec. measurement ND/FD technique

bump and uncertainty flux (anomaly) no impact on theta13

3.6. ν_e appearance and the quest for $\delta_{\rm CP}$

3.6.1. long baseline

T2K and NOVA (effect coupled to MH, NOVA if they publish)

nue appearance senstivity to delta CP (plot)

SK effect in atm due to delta

3.7. PMNS model: summary

data well described by 3nu oscillations (PMNS)

recent global fit (Concha/FL) table

experiment start to be sensitive to 3nu effects

4. Anomalies (SL)

LSND numu bar $\rightarrow$ nue bar $\rightarrow$ 4th nu

Miniboone inconclusive

reactor anomaly (controversy) - Ga anomaly

tension appearance/disappearance (CDHS Daya Bay Bugey)

3+1 models, bad fits

need for a clarification exp : test of reactor anomaly reactor(SOLID STEREO) + sources (SOX) + accelerators

need to understand the reactor spectrum

5. Perspectives for future experiments 20pg MZ

5.1. Existing projects: T2K NOVA

T2K statx10 + antinu data no MH

NOVA MH sensitivity (depends on delta)

(where do we add SK ?)

increased sensitivity to theta23

5.2. middle term

JUNO prec measurement of theta12 and Dm21
method NH/IH, critics Parke
depends on E exp resolution, not demonstrated
PINGU/ORCA discussion sensitivity MH (numu-¿numu vs showers)
INO distinguishes btw numu and numubar status ?

5.3. Long term: HyperKamiokande, DUNE

DUNE new technology LAr 40 kt new beam
decouples CP violation from MH with nu/nubar beam
HyperK 500 kt fiducial (finance ?) upgraded T2K beam
complementarity DUNE/HK

6. Conclusions

[1] Aartsen, M., et al., 2016. Neutrino oscillation studies with icecube-deepcore. Nuclear Physics B 908, 161 – 177, neutrino Oscillations: Celebrating the Nobel Prize in Physics 2015.
URL http://www.sciencedirect.com/science/article/pii/S0550321316300141

[2] Abe, K., et al., 2013. Evidence for the Appearance of Atmospheric Tau Neutrinos in Super-Kamiokande. Phys. Rev. Lett. 110 (18), 181802.

[3] Achar, C. V., et al., 1965. Detection of muons produced by cosmic ray neutrinos deep underground. Phys. Lett. 18, 196–199.

[4] Agafonova, N., et al., 2015. Discovery of τ Neutrino Appearance in the CNGS Neutrino Beam with the OPERA Experiment. Phys. Rev. Lett. 115 (12), 121802.

[5] Ahn, M. H., et al., 2006. Measurement of Neutrino Oscillation by the K2K Experiment. Phys. Rev. D74, 072003.

[6] Barr, G. D., Gaisser, T. K., Lipari, P., Robbins, S., Stanev, T., 2004. A Three - dimensional calculation of atmospheric neutrinos. Phys. Rev. D70, 023006.

[7] Battistoni, G., Ferrari, A., Montaruli, T., Sala, P. R., 2003. The FLUKA atmospheric neutrino flux calculation. Astropart. Phys. 19, 269–290, [Erratum: Astropart. Phys.19,291(2003)].

[8] Beavis, D., Carroll, A., Chiang, I., Apr. 1995. Long baseline neutrino oscillation experiment at the AGS. Tech. rep.

[9] Bernardini, P., Fogli, G., Lisi, E., Crescenzo, A. D., 2015. Proceedings of the neutrino oscillation workshop results from the opera experiment. Nuclear and Particle Physics Proceedings 265, 186 – 188.
URL http://www.sciencedirect.com/science/article/pii/S2405601415003892

[10] Fukuda, Y., et al., 1998. Evidence for oscillation of atmospheric neutrinos. Phys. Rev. Lett. 81, 1562–1567.

[11] Gaisser, T. K., Honda, M., 2002. Flux of atmospheric neutrinos. Ann. Rev. Nucl. Part. Sci. 52, 153–199.

[12] Honda, M., Kajita, T., Kasahara, K., Midorikawa, S., Jun 2011. Improvement of low energy atmospheric neutrino flux calculation using the jam nuclear interaction model. Phys. Rev. D 83, 123001.
URL http://link.aps.org/doi/10.1103/PhysRevD.83.123001

[13] Hosaka, J., et al., 2006. Three flavor neutrino oscillation analysis of atmospheric neutrinos in Super-Kamiokande. Phys. Rev. D74, 032002.

[14] Kopp, S. E., 2007. Accelerator neutrino beams. Physics Reports 439 (3), 101 – 159.
URL http://www.sciencedirect.com/science/article/pii/S0370157306004431

[15] Reines, F., Crouch, M. F., Jenkins, T. L., Kropp, W. R., Gurr, H. S., Smith, G. R., Sellschop, J. P. F., Meyer, B., 1965. Evidence for high-energy cosmic ray neutrino interactions. Phys. Rev. Lett. 15, 429–433.